

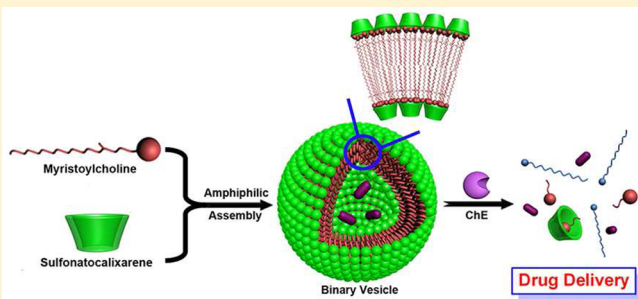
Cholinesterase-Responsive Supramolecular Vesicle

Dong-Sheng Guo, Kui Wang, Yi-Xuan Wang, and Yu Liu*

Department of Chemistry, State Key Laboratory of Elemento-Organic Chemistry, Nankai University, Tianjin 300071, People's Republic of China

Supporting Information

ABSTRACT: Enzyme-responsive, amphiphilic self-assembly represents one of the increasingly significant topics in biomaterials research and finds feasible applications to the controlled release of therapeutic agents at specific sites where the target enzyme is located. The supramolecular approach, using “superamphiphiles”, provides a smart way to fabricate drug delivery systems responsive to enzymatic catalysis. In this work based on the concept of supramolecular chemistry, we report an enzyme-responsive vesicle using *p*-sulfonatocalix[4]arene as the macrocyclic host and natural enzyme-cleavable myristoylcholine as the guest molecule. The complexation of *p*-sulfonatocalix[4]arene with myristoylcholine directs the formation of a supramolecular binary vesicle, which is dissipated by cholinesterase with high specificity and efficiency. Cholinesterase is a key protein overexpressed in Alzheimer's disease, and therefore, the present system may have potential for the delivery of Alzheimer's disease drugs.



INTRODUCTION

Enzymes play essential roles in a lot of biochemical processes, and often aberrations in the enzyme expression level have been associated with many diseases.¹ As an appealing quest for therapeutic purposes, enzyme-responsive assemblies have gained considerable attention in the fields of biotechnology, diagnostics, and drug delivery systems,² where the entrapped drugs are released from self-assembled carriers triggered by specific enzymatic reactions.³ Compared to approaches with other external stimuli, such as temperature, pH, and light, the enzyme-based approach represents an elegant biocompatible method of high sensitivity and selectivity for targeted delivery of therapeutics to the enzyme-overexpression sites. Essentially all of the drug delivery vehicles hitherto employed are amphiphilic in nature, including micelles, vesicles, nanoparticles, and hydrogels. Fabrication of enzyme-responsive drug delivery systems should therefore address two formidable challenges: (1) enzymes convert self-assembling amphiphilic substrates into nonassembling nonamphiphilic products (vice versa); (2) tedious covalent syntheses are always involved in preparing desired amphiphiles, which will not only reduce their biocompatibility but also affect the enzyme activity and specificity due to suboptimal reactivity of the enzyme to the modified substrates. In this regard, the supramolecular approach is expected as a smart strategy for bottom-up fabrication, where tectons are held together with reversible noncovalent interactions. However, to the best of our knowledge, the concept of “superamphiphiles”,⁴ amphiphiles that are generated by noncovalent synthesis, has been much less frequently engaged in building supramolecular enzyme-triggered drug delivery, as well as pattern-sensing systems.⁵ Up to now, several kinds of noncovalent interactions have been

used to build superamphiphiles, including hydrogen-bonding, charge-transfer, and $\pi\cdots\pi$ interactions, among others.⁶ These frequently employed noncovalent interactions are not always effective for making assemblies in aqueous media, and many of the assemblies formed lack biocompatibility, which is essential for applications in the field of biotechnology. The host–guest complexation events based on cyclodextrin, sulfonatocalixarene, and cucurbituril occur commonly in aqueous media, and therefore, the use of macrocyclic receptors is particularly advantageous in constructing water-soluble supramolecular architectures.⁷ Moreover, such macrocycles have been shown to be very biocompatible.⁸ Consequently, the construction of superamphiphiles through host–guest recognition is of particular interest and importance in fundamental research and practical application of biotechnology and medicine, although only a limited amount of endeavor has been devoted so far to this research area.⁹

We present here a new strategy of building enzyme-responsive supramolecular vesicles as an operational targeted drug delivery system, where host–guest complexes act as superamphiphiles, avoiding the tedious covalent syntheses and substrate modification. As the initial part of our ongoing program, biocompatible *p*-sulfonatocalix[4]arene (SC4A)^{8b–d} and natural myristoylcholine were employed as the macrocyclic host and enzyme-cleavable guest, respectively. Our design proposed herein combines the following three advantages: (1) the complexation of SC4A with myristoylcholine lowers its critical aggregation concentration (CAC) pronouncedly to

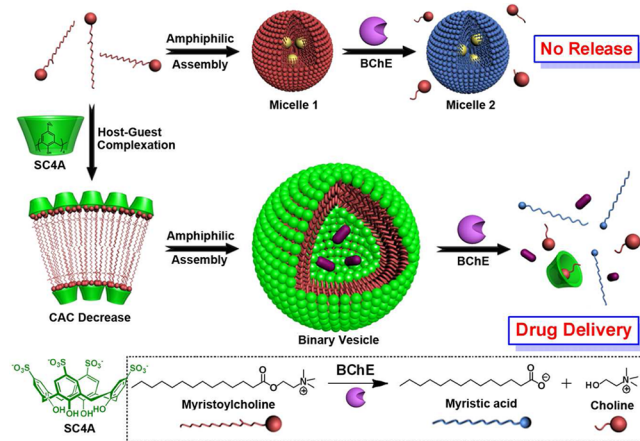
Received: April 5, 2012

Revised: May 21, 2012

Published: June 11, 2012

form a binary vesicle;¹⁰ (2) cholinesterases (acetylcholinesterase (AChE) and butyrylcholinesterase (BChE)) convert myristoylcholine to myristic acid and choline with unparalleled specificity;^{5b,11} (3) SC4A binds nonamphiphilic choline but not amphiphilic myristic acid, leading to the complexed vesicle being dissipated (Scheme 1).¹² Recently, the interaction of

Scheme 1. Schematic Illustration of Amphiphilic Assemblies of Myristoylcholine in the Absence and Presence of SC4A^a



^aFree myristoylcholine self-assembles into micelle 1 at higher concentration (>2.5 mM). Micelle 1 is not dissipated but transferred into micelle 2 accompanied by the BChE reaction (the hydrophilic–hydrophobic balance is not lost from myristoylcholine substrate to myristic acid product), and then, the hydrophobic drugs (yellow small spheres) cannot be released from the micelles. Upon addition of SC4A, the CAC of myristoylcholine decreases by 2 orders of magnitude, and the host–guest complex self-assembles into a binary vesicle at lower concentration (< 0.1 mM). The vesicle can be specifically dissipated by BChE, leading to the release of entrapped hydrophilic drugs (purple rods).

cholinesterase with supramolecular assemblies derived from myristoylcholine and anionic molecules has been reported.¹¹ Zhu et al.^{11a} and Li et al.^{11b} have shown that the heteroaggregates can be used in convenient fluorometric or colorimetric AChE sensing and its inhibitor screening. Especially, Zhang et al. have very recently reported a cholinesterase-responsive spherical aggregate as a carrier for drug delivery.^{5b} However, to the best of our knowledge, the construction of cholinesterase-responsive vesicles has not been reported so far.

Vesicles are not only ubiquitous building blocks in living systems but also highly useful, often essential, components of artificial biomimetic systems, light-harvesting systems, micro-reactors, and particularly drug/gene delivery systems.¹³ In contrast to the solid micelles that are suitable to entrap hydrophobic drugs, the hollow vesicles prefer to load hydrophilic drugs into their inner cavities. Notably, the overexpression of cholinesterase has been implicated for Alzheimer's disease,¹⁴ and the current rational clinical treatment is mainly based on the cholinesterase inhibitors, most of which are hydrophilic, as was the case with the first Alzheimer's disease drug tacrine. The present vesicle system is therefore potentially applicable to the controlled release of Alzheimer's disease drugs, following our previous tandem cholinesterase assays and screening for inhibitors.¹⁵

RESULTS AND DISCUSSION

Myristoylcholine was employed as it is a soft antimicrobial agent and can be used in drug delivery systems.¹⁶ Although myristoylcholine is a natural enzyme-active molecule, it is defective in fabricating an enzyme-responsive assembly independently as the CACs of the substrate and product are similar (Scheme 1). Both myristoylcholine and myristic acid form micelles with CACs of 2.5 and 4.5 mM, respectively.^{11a,17} Dramatically, the CAC value of myristoylcholine can be pronouncedly decreased by the complexation of SC4A, while that of myristic acid remains unchangeable as there is no complexation of SC4A. The CAC decrease of myristoylcholine in the presence of SC4A was measured by monitoring the dependence of the optical transmittance around 450 nm on the concentration of myristoylcholine. In the absence of SC4A, the optical transmittance of myristoylcholine at 450 nm shows no appreciable change as the concentration increases from 0.005 to 0.100 mM (Figure S1, Supporting Information). This indicates that myristoylcholine cannot aggregate in this concentration region, in nice agreement with the previous results measured by calorimetry and surface tension.^{11a,17b} Upon addition of SC4A, the optical transmittance decreases gradually with increasing myristoylcholine concentration as a result of amphiphilic assembly. The complexation-induced CAC can therefore be obtained according to the plot of optical transmittance at 450 nm versus the concentration of myristoylcholine: ca. 0.02–0.03 mM (Figure S2, Supporting Information). This means that the CAC of myristoylcholine decreases significantly by a factor of ca. 100 due to the complexation with SC4A. Note that SC4A did not show any tendency to self-aggregate in aqueous solution.¹⁸ Control experiments show that replacement of SC4A by its building subunit 4-phenolsulfonic sodium could not induce the reduction of CAC (Figure S3, Supporting Information), indicating that a host–guest complexation of SC4A with myristoylcholine is undoubtedly the critical factor leading to an amphiphilic assembly, where the electrostatic interactions between negative sulfonate groups and positive quaternary ammonium groups reinforce the complex stability.

It is a prerequisite to determine the best molar ratio between SC4A and myristoylcholine for constructing a robust amphiphilic assembly. Figure 1 shows the optical transmittance spectra (top) and the plot of transmittance at 450 nm as a function of the concentration of SC4A added to a myristoylcholine solution at fixed 0.10 mM (bottom). The transmittance at 450 nm first decreased rapidly with increasing SC4A concentration until the minimum was reached at a SC4A/myristoylcholine ratio of 0.1 and then gradually increased thereafter to approach a quasi-plateau. The rapid decrease indicates the formation of a higher order complex of SC4A with myristoylcholine, eventually leading to an amphiphilic assembly, which is however disassembled upon further addition of SC4A to afford a simple 1:1 inclusion complex. The inflection appears at a SC4A/myristoylcholine molar ratio of 0.1, which means that, in the present SC4A–myristoylcholine system, the best mixing ratio for the amphiphilic assembly is 1:10 SC4A:myristoylcholine.¹⁹

The solution of SC4A + myristoylcholine exhibited a clear Tyndall effect (Figure 2a), indicating the existence of abundant nanoparticles. A similar phenomenon was not observed for the solution of free myristoylcholine, revealing that free myristoylcholine cannot form nanoscale aggregates under the same conditions. Furthermore, dynamic laser scattering (DLS),

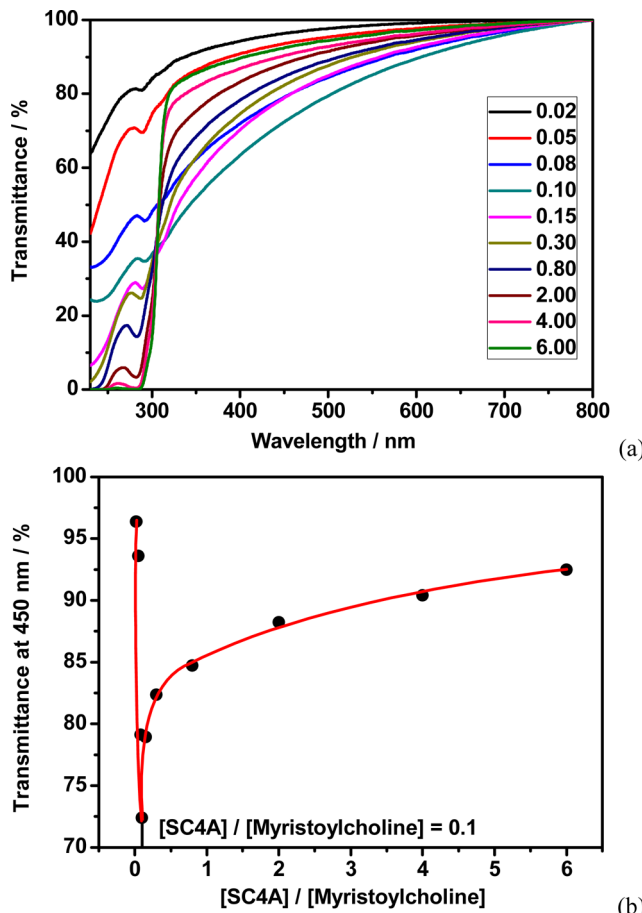


Figure 1. (a) Optical transmittance of myristoylcholine (0.10 mM) by increasing the concentration of SC4A from 0.002 mM (0.02 equiv) to 0.60 mM (6.00 equiv) at 25 °C in water. (b) Dependence of the optical transmittance at 450 nm on the SC4A concentration with a fixed myristoylcholine concentration of 0.10 mM at 25 °C.

transmission electron microscopy (TEM), and scanning electron microscopy (SEM) were employed to identify the self-assembly morphology and size of the SC4A + myristoylcholine superamphiphile. The DLS examinations revealed that the SC4A–myristoylcholine complex forms spectacular assemblies with a narrow size distribution, giving an average diameter of 194 nm at a scattering angle of 90° (Figure 2a). The TEM image at an accelerating voltage of 100 keV (Figure S4, Supporting Information) and SEM image (Figure 2b) show the spherical morphology with a diameter ranging from 90 to 200 nm. The measured diameters of the aggregates exceed the corresponding extended molecular length, suggesting that these aggregates are vesicular entities rather than simple micelles.²⁰ The formation of vesicles was convincingly validated by cryo-TEM (Figure S5, Supporting Information) as well as TEM (Figure 2d) and high-resolution TEM (Figure 2c) images at an accelerating voltage of 200 keV, showing the hollow spherical morphology. From the distinguishably dark periphery and the light central parts, we obtained the thickness of the bilayer membrane as ca. 4 nm, which is of the same order of magnitude as the sum of two myristoylcholine lengths and two SC4A heights. The light scattering studies on a monodisperse vesicle sample of SC4A + myristoylcholine revealed that the radius of gyration ($R_g = 175$ nm) and hydrodynamic radius ($R_h = 153$ nm) are almost identical ($\rho (R_g/R_h) = 1.1$), which is also

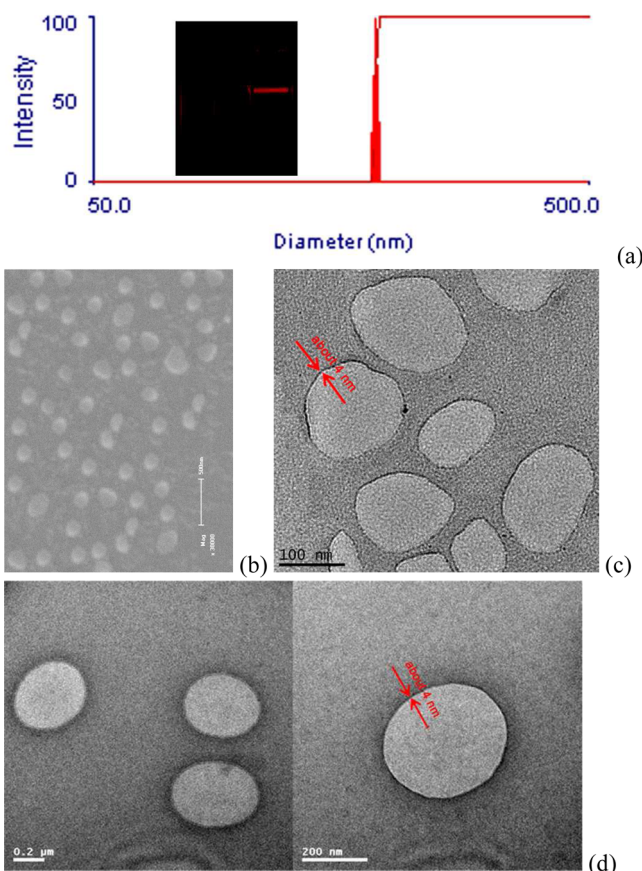


Figure 2. (a) DLS data of the SC4A + myristoylcholine assembly. Inset: Photos showing the Tyndall effect of free myristoylcholine (left) and the SC4A–myristoylcholine complex (right). (b) SEM, (c) high-resolution TEM, and (d) TEM images of the SC4A + myristoylcholine assembly. [Myristoylcholine] = 0.10 mM, and [SC4A] = 0.01 mM.

characteristic of vesicles.²¹ Combining all the aforementioned results, we may conclude that the supramolecular binary vesicle is formed as schematically illustrated in Scheme 1. The hydrophobic alkyl chains in myristoylcholine are packed together, and the inner- and outer-layer surfaces consist of hydrophilic phenol OH groups of SC4A, which are exposed to the aqueous solution. SC4A and myristoylcholine are connected together by host–guest interactions. This model was also confirmed by NMR results (Figure S6, Supporting Information). The resulting binary vesicle is stable, and the vesicular structure can be maintained at least over 24 h (Figure S9, Supporting Information).

The pH value for this SC4A + myristoylcholine system was determined as 6.8, which is in the range of physiological pH for enzymatic reactions. The disassembly process induced by enzyme was monitored using optical transmittance studies. Both AChE and BChE are specific enzymes to cleave myristoylcholine; however, the overexpression of BChE is implicated in the exacerbation of Alzheimer's disease,¹⁴ and therefore, BChE was employed in this work. BChE was added to the SC4A + myristoylcholine solution, ca. 0.5 U/mL, which is comparable with the average amount of cholinesterase present in a healthy adult. We were gratified to find a systematic increase with time in the optical transmittance at 450 nm, which finally reached more than 96% after 3 h (Figure 3a), revealing that almost all the vesicular assemblies disappeared in about 3 h. More powerful evidence for the disassembly of the

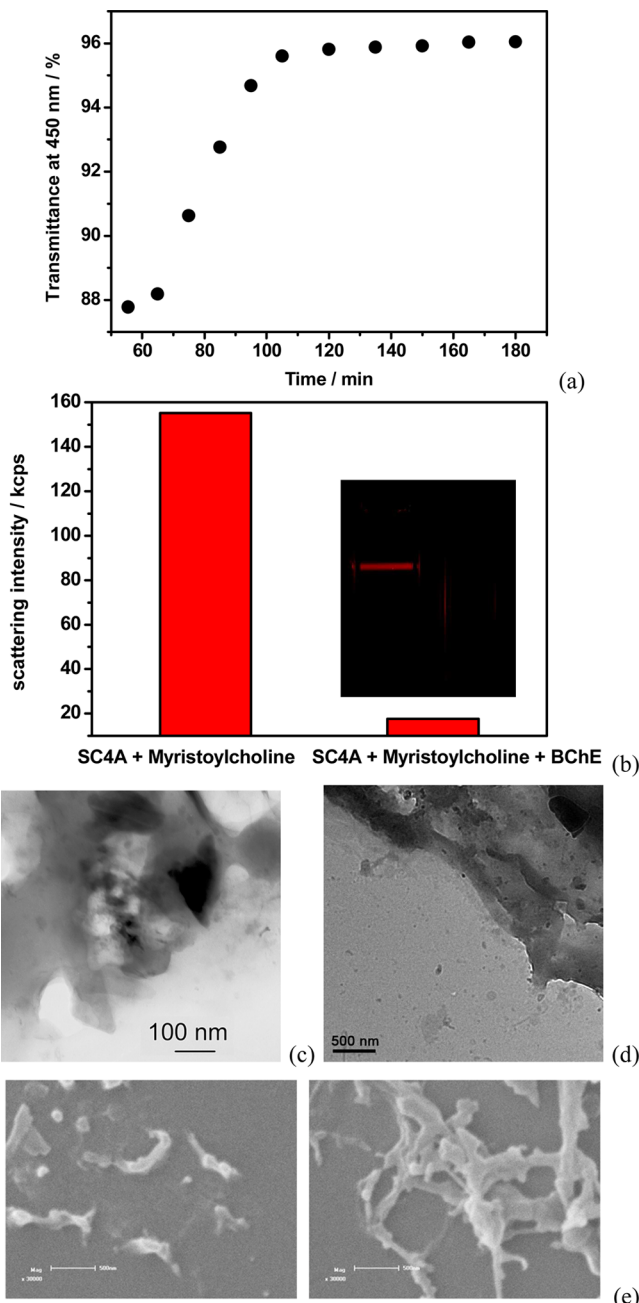


Figure 3. (a) Dependence of the optical transmittance of SC4A + myristoylcholine aggregation at 450 nm on time in the presence of BChE. (b) Scattering intensity of the SC4A + myristoylcholine assembly before (left) and after (right) addition of BChE for 3 h. Inset: Tyndall effect of the SC4A + myristoylcholine assembly before (left) and after (right) addition of BChE for 3 h. (c) TEM, (d) high-resolution TEM, and (e) SEM images of the SC4A + myristoylcholine assembly after addition of BChE for 3 h. [Myristoylcholine] = 0.10 mM, [SC4A] = 0.01 mM, and [BChE] = 0.5 U/mL.

vesicles upon addition of BChE comes from DLS measurements, showing that the scattering intensity decreases pronouncedly from 155.3 to 17.7 kcps in 3 h, accompanied by the disappearance of the Tyndall effect (Figure 3b). TEM (Figure 3c), high-resolution TEM (Figure 3d), and SEM (Figure 3e) images also show that hardly any vesicular morphology was observed after BChE treatment. Furthermore, we found that the formation and enzyme-triggered disassembly

of SC4A + myristoylcholine vesicles can also be achieved in normal saline (Figure S11, Supporting Information).

Mass spectrum measurements were also performed to further demonstrate the enzymatic cleavage of the ester bonds of myristoylcholine in the supramolecular vesicles. Figure S12 (Supporting Information) shows mass spectra of the supramolecular vesicle at different time points after addition of BChE. The peak at 314, assigned to [myristoylcholine]⁺, was obviously weakened after 5 h, and almost disappeared 12.5 h later, indicating that all of the ester bonds had been cleaved. The time for the complete disassembly of the supramolecular vesicles is much shorter than that for the complete cleavage of the ester bonds, since almost all vesicles were dissipated even when some myristoylcholine molecules remained with a concentration lower than the CAC.^{5a} The rate for the cholinesterase-responsive disassembly is related to the concentration of the enzyme added, and increasing amount of enzyme would accelerate the disassembly (Figure S13, Supporting Information). Important to note, the hydrolysis rate of the binary vesicle by BChE is much slower than that of free myristoylcholine because there is a dynamic equilibrium between the assembled and unassembled states of myristoylcholine, and BChE attacks only the free species.

To prove that the protein BChE itself is not a factor contributing to the disassembly of the vesicle, a control experiment was carried out in which the same amount of denatured BChE (treated in boiling water for 1 h) was added to the SC4A + myristoylcholine solution. No appreciable change over time was observed in either the optical transmittance at 450 nm or the Tyndall effect (Figure 4). Thus, the result clearly

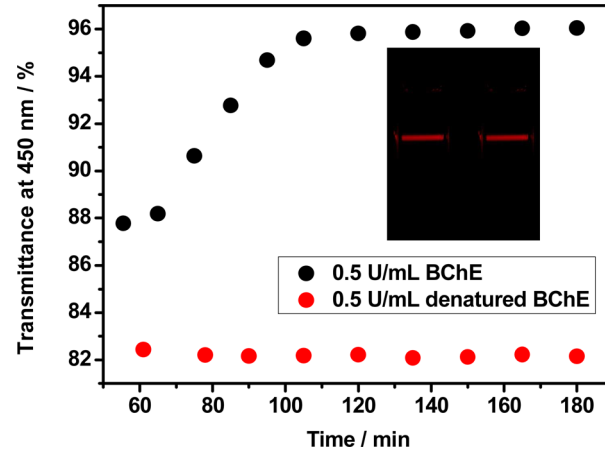


Figure 4. (a) Dependence of the optical transmittance of SC4A + myristoylcholine aggregation at 450 nm on time in the presence of 0.5 U/mL BChE and denatured BChE. Inset: Tyndall effect of the SC4A + myristoylcholine aggregation before (left) and after (right) addition of 0.5 U/mL denatured BChE for 3 h. [Myristoylcholine] = 0.10 mM, and [SC4A] = 0.01 mM.

eliminates the possibility of the enzyme protein itself being a factor of disassembly. To investigate the specificity of the cholinesterase-responsive disassembly, the optical transmittance results for the binary vesicle upon addition of other enzymes such as calf intestinal alkaline phosphatase (CIAP), exonuclease I (Exo I), and glucose oxidase (GOx) were recorded. The concentration of each enzyme was kept at 0.5 U/mL. As shown in Figure S15 (Supporting Information), in the presence of CIAP/Exo I/GOx, there was no significant change over time in

either the optical transmittance at 450 nm or the Tyndall effect, demonstrating that this enzyme-responsive vesicle exhibits excellent specificity toward cholinesterase.

It is reasonable to expect that the disassembly would trigger a concomitant release of any hydrophilic guest molecule sequestered within the vesicular interior. To test this, the trisodium salt of 8-hydroxypyrene-1,3,6-trisulfonic acid (HPTS) as a model molecule was loaded into the vesicles. Excess HPTS was removed by dialysis. The dialysis process also revealed that the SC4A + myristoylcholine binary vesicle is sufficiently stable in an aqueous medium. The release kinetics of HPTS with and without addition of BChE was evaluated through fluorescence emission spectroscopy. As shown in Figure 5a, a very low release of entrapped HPTS was observed

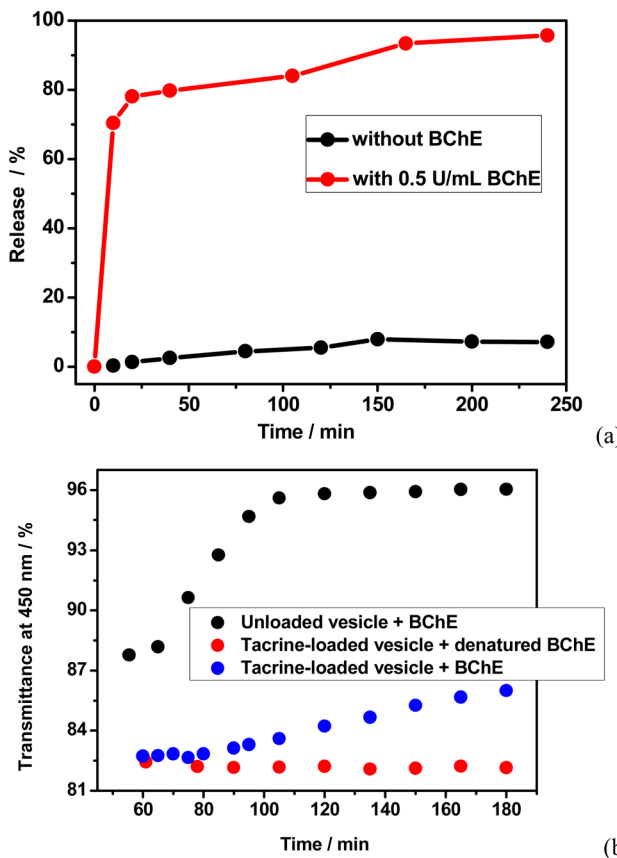


Figure 5. (a) Release of HPTS entrapped in the supramolecular SC4A + myristoylcholine vesicle with and without BChE. (b) Dependence of the optical transmittance of the unloaded vesicle at 450 nm on time in the presence of 0.5 U/mL BChE and dependence of the optical transmittance of the tacrine-loaded vesicle at 450 nm on time in the presence of 0.5 U/mL BChE and denatured BChE. [Myristoylcholine] = 0.10 mM, and [SC4A] = 0.01 mM.

over periods of 4 h, indicating that the vesicles are highly stable toward leakage at room temperature. However, the release rate was significantly enhanced when the vesicles were treated with BChE, demonstrating the cholinesterase-triggered release of the binary vesicle. About 80% HPTS was released in the first 20 min, reaching almost 100% in 4 h. In addition, almost no HPTS release was observed for the vesicle solution treated with other enzymes such as GOx, as expected, and more enzyme would result in an accelerated or enhanced release (Figure S17, Supporting Information). This phenomenon renders the present supramolecular vesicle an intriguing targeted-delivery

carrier of drugs, which encapsulates drug molecules inside, protects the active ingredient from premature degradation, and releases them when encountered with cholinesterase, in particular at the tissue where cholinesterase is overexpressed.

We further loaded tacrine, a typical water-soluble cholinesterase inhibitor for the treatment of Alzheimer's disease, into the vesicle. The presence of 0.5 U/mL BChE disassembles the tacrine-loaded vesicle, while denatured BChE does not, which indicates that the loaded tacrine can only be released upon cholinesterase-triggered vesicle disassembly (Figure 5b). More importantly, the tacrine-loaded vesicle underwent only a partial disassembly, which is different from the complete disassembly of the free vesicle. The effect not only reflects that the released tacrine has played a therapeutic effect in inhibiting the activity of cholinesterase, but also implies that excessive tacrine cannot be further released after all the enzymatic activities were inhibited, which eliminates any potential side effects caused by excessive tacrine release. Therefore, such a controlled release system will enhance the drug efficacy, while simultaneously minimizing the undesired side effects, if any.

Finally, basic cell experiments were carried out to evaluate the cellular toxicity of the supramolecular binary vesicle. LO2 cells (normal human liver cell line) were incubated with and without SC4A + myristoylcholine vesicle ([SC4A] = 0.01 mM, [myristoylcholine] = 0.1 mM), and the number of living cells in each group was recorded from day 1 to day 4. As shown in Figures 6 and S19 (Supporting Information), we found that the number of living cells in the vesicle group was statistically equivalent to that in the blank group ($P > 0.05$) every day and the morphology of living cells in the vesicle group is also similar to that in the blank group. All these results suggest that the SC4A + myristoylcholine vesicle employed in this work is

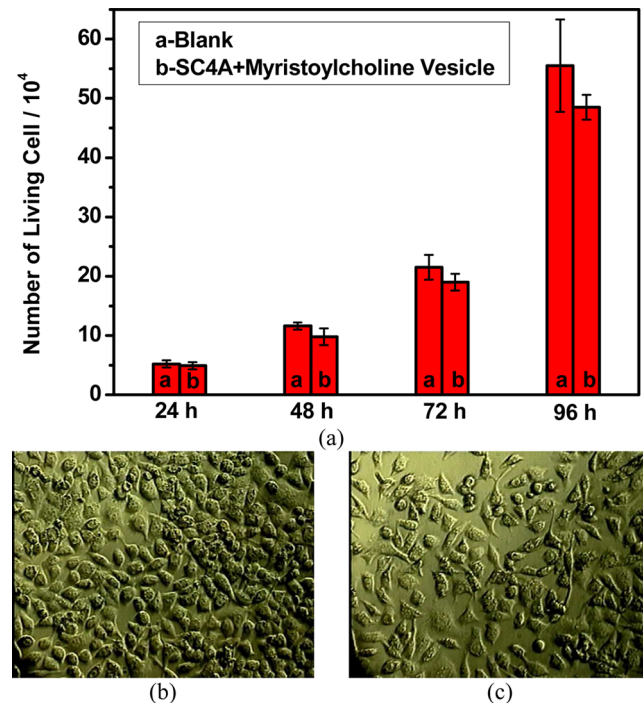


Figure 6. (a) Number of living LO2 cells in the blank group and after treatment with SC4A + myristoylcholine vesicle from day 1 to day 4. Images of living LO2 cells in the blank (b) and SC4A + myristoylcholine vesicle (c) groups after 72 h.

practically nontoxic and therefore is an ideal carrier for drug delivery.

CONCLUSION

In conclusion, we have successfully constructed an enzyme-responsive supramolecular vesicle as an operational targeted drug delivery system, based on the concept of host–guest chemistry. By taking advantage of the dynamic equilibrium characteristics of noncovalent interactions, the self-assembled vesicle was successfully disintegrated by the action of the enzyme. Although the cleavage rate may be reduced, it is certainly advantageous over the covalent modification of substrates, which often results in a loss of enzyme recognition. The present binary vesicle from SC4A and myristoylcholine exhibits highly specific and efficient responsiveness to cholinesterase. An enzyme-induced cleavage of myristoylcholine triggers a cascade of events, loss of the hydrophilic–hydrophobic balance of the binary superamphiphile, disassembly of the vesicle, and tandem release of entrapped drugs. We believe that this approach can be extended to various enzyme-triggered self-assembled materials, showing feasible applications in the controlled release at specific enzyme sites. Further *in vivo* studies are currently ongoing.

EXPERIMENTAL SECTION

Materials Preparation. Myristoylcholine chloride, BChE (from equine serum, 246 U/mg), HPTS, and tacrine were purchased from Sigma-Aldrich. Choline and GOx were purchased from Aladdin. CIAP and Exo I were purchased from Takara. Sodium myristate was purchased from TCI, and 4-phenolsulfonic sodium was purchased from Acros. All of these were used without further purification. SC4A was synthesized and purified according to the procedures reported previously²² and identified by ¹H NMR spectroscopy in D₂O, performed on a Varian 300 spectrometer, and elemental analysis, performed on a Perkin-Elmer 2400C instrument.

HPTS-Loaded Vesicles. HPTS-loaded vesicles were prepared as follows: A certain amount of HPTS was added to a solution containing SC4A and myristoylcholine, and then some water was added until the volume of the solution reached 25 mL. The ultimate concentrations of HPTS, myristoylcholine, and SC4A were 0.01, 0.10, and 0.01 mM, respectively. Subsequently, the prepared HPTS-loaded vesicles were purified by dialysis (molecular weight cutoff 3500) in distilled water several times until the water outside the dialysis tube exhibited negligible HPTS fluorescence.

UV/Vis Spectra. The optical transmittance of the aqueous solution was measured in a quartz cell (light path 10 mm) on a Shimadzu UV-3600 spectrophotometer equipped with a PTC-348WI temperature controller.

Fluorescence Spectra. Steady-state fluorescence spectra were recorded in a conventional quartz cell (light path 10 mm) on a Varian Cary Eclipse equipped with a Varian Cary single-cell Peltier accessory to control the temperature ($\lambda_{\text{ex}} = 339.0$ nm, bandwidth(ex) 2.5 nm, bandwidth(em) 5.0 nm).

TEM, High-Resolution TEM, and SEM Experiments. TEM images were recorded on a Philips EM400st TEM operating at an accelerating voltage of 100 keV and on a Philips Tecnai G2 20S-TWIN microscope operating at an accelerating voltage of 200 keV. High-resolution TEM images were acquired using a Tecnai 20 high-resolution transmission electron microscope operating at an accelerating voltage of 200 keV. The sample for TEM measurements was prepared by dropping the solution onto a copper grid. The grid was then air-dried. SEM images were recorded on a Hitachi S-3500N scanning electron microscope. The sample for SEM measurements was prepared by dropping the solution onto a coverslip, followed by evaporating the liquid in air.

Cryo-TEM Experiments. Cryo-TEM was performed on an FEI Tecnai 20. A drop of solution was dropped onto a copper grid coated

with a holey carbon support film. After 15 s, the water was removed by paper. The copper grid was immersed into liquid C₂H₆ immediately and then transferred into liquid nitrogen for further observation.

DLS Measurements. The sample solution for DLS measurements was prepared by filtering the solution through a 450 nm Millipore filter into a clean scintillation vial. The samples were examined on a laser light scattering spectrometer (BI-200SM) equipped with a digital correlator (TurboCorr) at 532 nm at a scattering angle of 90°. The hydrodynamic radius (R_h) was determined by dynamic light scattering experiments, and the radius of gyration (R_g) was obtained from static light scattering data at different scattering angles.

Cell Experiments. LO2 cells (normal human liver cell line) were seeded in a clear 24-well plate at a density of 2×10^4 cells/well in 1000 μL of complete RPMI 1640 and 10% fetal calf serum (FCS) and grown for 6 h with 5% CO₂ at 37 °C. LO2 cells were subsequently incubated with and without the SC4A + myristoylcholine vesicle. The ultimate concentrations of SC4A and myristoylcholine were 0.01 and 0.10 mM, respectively. After another 24, 48, 72, and 96 h of incubation, the number of living cells in every group was measured. The number of living cells is expressed as the mean \pm standard deviation, and a *t* test was used for statistical analysis of the data. Differences were considered statistically significant when the *P* value was less than 0.05.

ASSOCIATED CONTENT

S Supporting Information

Experimental procedures and supporting figures. This material is available free of charge via the Internet at <http://pubs.acs.org>.

AUTHOR INFORMATION

Corresponding Author

yiliu@nankai.edu.cn

Notes

The authors declare no competing financial interest.

ACKNOWLEDGMENTS

We thank the 973 Program (Grant 2011CB932502) and National Natural Science Foundation of China (Grants 20932004 and 21172119) for financial support.

REFERENCES

- (a) Samantaray, S.; Sharma, R.; Chattopadhyaya, T.; Gupta, K. S. D.; Ralhan, R. *J. Cancer Res. Clin. Oncol.* **2004**, *130*, 37–44.
- (b) Spaltenstein, A.; Kamierski, W. M.; Miller, J. F.; Samano, V. *Curr. Top. Med. Chem.* **2005**, *5*, 1589–1607. (c) Guo, T.; Hobbs, D. W. *Curr. Med. Chem.* **2006**, *13*, 1811–1829.
- (2) (a) Um, S. H.; Lee, J. B.; Park, N.; Kwon, S. Y.; Umbach, C. C.; Luo, D. *Nat. Mater.* **2006**, *5*, 797–801. (b) Williams, R. J.; Smith, A. M.; Collins, R.; Hodson, N.; Das, A. K.; Uljin, R. V. *Nat. Nanotechnol.* **2009**, *4*, 19–24. (c) Morimoto, N.; Ogino, N.; Narita, T.; Kitamura, S.; Akiyoshi, K. *J. Am. Chem. Soc.* **2007**, *129*, 458–459. (d) Amir, R. J.; Zhong, S.; Pochan, D. J.; Hawker, C. J. *J. Am. Chem. Soc.* **2009**, *131*, 13949–13951. (e) Alemdaroglu, F. E.; Wang, J.; Börsch, M.; Berger, R.; Herrmann, A. *Angew. Chem., Int. Ed.* **2008**, *47*, 974–976. (f) Chien, M.-P.; Rush, A. M.; Thompson, M. P.; Gianneschi, N. C. *Angew. Chem., Int. Ed.* **2010**, *49*, 5076–5080.
- (3) (a) Yang, Z. M.; Liang, G. L.; Xu, B. *Acc. Chem. Res.* **2008**, *41*, 315–326. (b) Yang, Z. M.; Liang, G. L.; Wang, L.; Xu, B. *J. Am. Chem. Soc.* **2006**, *128*, 3038–3043. (c) Azagarsamy, M. A.; Sokkalingam, P.; Thayumanavan, S. *J. Am. Chem. Soc.* **2009**, *131*, 14184–14185. (d) Raghupathi, K. R.; Azagarsamy, M. A.; Thayumanavan, S. *Chem.—Eur. J.* **2011**, *17*, 11752–11760. (e) Uljin, R. V. *J. Mater. Chem.* **2006**, *16*, 2217–2225. (f) Thornton, P. D.; Mart, R. J.; Uljin, R. V. *Adv. Mater.* **2007**, *19*, 1252–1256. (g) Lutolf, M. P.; Hubbell, J. A. *Nat. Biotechnol.* **2005**, *23*, 47–55. (h) Kühnle, H.; Börner, H. G. *Angew. Chem., Int. Ed.* **2009**, *48*, 6431–6434.

- (4) (a) Wang, Y.; Xu, H.; Zhang, X. *Adv. Mater.* **2009**, *21*, 2849–2864. (b) Zhang, X.; Wang, C. *Chem. Soc. Rev.* **2011**, *40*, 94–101.
- (5) (a) Wang, C.; Chen, Q.; Wang, Z.; Zhang, X. *Angew. Chem., Int. Ed.* **2010**, *49*, 8612–8615. (b) Xing, Y.; Wang, C.; Han, P.; Wang, Z.; Zhang, X. *Langmuir* **2012**, *28*, 6032–6036. (c) Savariar, E. N.; Ghosh, S.; González, D. C.; Thayumanavan, S. *J. Am. Chem. Soc.* **2008**, *130*, 5416–5417.
- (6) (a) Kimizuka, N.; Kawasaki, T.; Hirata, K.; Kunitake, T. *J. Am. Chem. Soc.* **1998**, *120*, 4094–4104. (b) Zhang, X.; Chen, Z.; Würthner, F. *J. Am. Chem. Soc.* **2007**, *129*, 4886–4887. (c) Wang, Y.; Ma, N.; Wang, Z.; Zhang, X. *Angew. Chem., Int. Ed.* **2007**, *46*, 2823–2826. (d) Wang, C.; Yin, S.; Chen, S.; Xu, H.; Wang, Z.; Zhang, X. *Angew. Chem., Int. Ed.* **2008**, *47*, 9049–9052. (e) Ko, Y. H.; Kim, E.; Hwang, I.; Kim, K. *Chem. Commun.* **2007**, 1305–1315. (f) Bize, C.; Garrigues, J.-C.; Blanzat, M.; Rico-Lattes, I.; Bistri, O.; Collasson, B.; Reinaud, O. *Chem. Commun.* **2010**, *46*, 586–588.
- (7) (a) Kim, K.; Selvapalam, N.; Ko, Y. H.; Park, K. M.; Kim, D.; Kim, J. *Chem. Soc. Rev.* **2007**, *36*, 267–279. (b) Liu, Y.; Chen, Y. *Acc. Chem. Res.* **2006**, *39*, 681–691. (c) Harada, A.; Takashima, Y.; Yamaguchi, H. *Chem. Soc. Rev.* **2009**, *38*, 875–882. (d) Guo, D.-S.; Liu, Y. *Chem. Soc. Rev.* **2012**, in press.
- (8) (a) Uekama, K.; Hirayama, F.; Irie, T. *Chem. Rev.* **1998**, *98*, 2045–2076. (b) Perret, F.; Lazar, A. N.; Coleman, A. W. *Chem. Commun.* **2006**, *42*, 2425–2438. (c) Perret, F.; Coleman, A. W. *Chem. Commun.* **2011**, *47*, 7303–7319. (d) Wang, K.; Guo, D.-S.; Zhang, H.-Q.; Li, D.; Zheng, X.-L.; Liu, Y. *J. Med. Chem.* **2009**, *52*, 6402–6412. (e) Uzunova, V. D.; Cullinane, C.; Brix, K.; Nau, W. M.; Day, A. I. *Org. Biomol. Chem.* **2010**, *8*, 2037–2042.
- (9) (a) Jeon, Y. J.; Bharadwaj, P. K.; Choi, S. W.; Lee, J. W.; Kim, K. *Angew. Chem., Int. Ed.* **2002**, *41*, 4474–4476. (b) Jing, B.; Chen, X.; Wang, X.; Yang, C.; Xie, Y.; Qiu, H. *Chem.—Eur. J.* **2007**, *13*, 9137–9142. (c) Zeng, J.; Shi, K.; Zhang, Y.; Sun, X.; Zhang, B. *Chem. Commun.* **2008**, 3753–3755. (d) Yan, Q.; Yuan, J.; Cai, Z.; Xin, Y.; Kang, Y.; Yin, Y. *J. Am. Chem. Soc.* **2010**, *132*, 9268–9270.
- (10) (a) Wang, K.; Guo, D.-S.; Liu, Y. *Chem.—Eur. J.* **2010**, *16*, 8006–8011. (b) Wang, K.; Guo, D.-S.; Wang, X.; Liu, Y. *ACS Nano* **2011**, *5*, 2880–2894. (c) Basilio, N.; García-Río, L. *Chem.—Eur. J.* **2009**, *15*, 9315–9319. (d) Francisco, V.; Basilio, N.; García-Río, L.; Leis, J. R.; Maques, E. F.; Vázquez-Vázquez, C. *Chem. Commun.* **2010**, *46*, 6551–6553. (e) Basilio, N.; Martín-Pastor, M.; García-Río, L. *Langmuir* **2012**, *28*, 6561–6568.
- (11) (a) Wang, M.; Gu, X.; Zhang, G.; Zhang, D.; Zhu, D. *Anal. Chem.* **2009**, *81*, 4444–4449. (b) Li, Y.; Bai, H.; Li, C.; Shi, G. *ACS Appl. Mater. Interfaces* **2011**, *3*, 1306–1310.
- (12) It is well-established that SC4A exhibits especially strong binding affinity and high molecular selectivity toward organic cations; see, for example: Guo, D.-S.; Wang, K.; Liu, Y. *J. Inclusion Phenom. Macrocyclic Chem.* **2008**, *62*, 1–21.
- (13) (a) Mueller, A.; O'Brien, D. F. *Chem. Rev.* **2002**, *102*, 727–757. (b) Vriezema, D. M.; Aragonès, M. C.; Elemans, J. A. A. W.; Cornelissen, J. J. L. M.; Rowan, A. E.; Nolte, R. J. M. *Chem. Rev.* **2005**, *105*, 1445–1489. (c) Zhou, S.; Burger, C.; Chu, B.; Sawamura, M.; Nagahama, N.; Togano, M.; Hackler, U. E.; Isobe, H.; Nakamura, E. *Science* **2001**, *291*, 1944–1947. (d) Zhang, X.; Rehm, S.; Safont-Sempere, M. M.; Würthner, F. *Nat. Chem.* **2009**, *1*, 623–629.
- (14) (a) Whitehouse, P. J.; Price, D. L.; Struble, R. G.; Clark, A. W.; Coyle, J. T.; Delon, M. R. *Science* **1982**, *215*, 1237–1239. (b) Koo, E. H.; Lansbury, P. T.; Kelly, J. W. *Proc. Natl. Acad. Sci. U.S.A.* **1999**, *96*, 9989–9990. (c) Selkoe, D. J. *Physiol. Rev.* **2001**, *81*, 741–746.
- (15) Guo, D.-S.; Uzunova, V. D.; Su, X.; Liu, Y.; Nau, W. M. *Chem. Sci.* **2011**, *2*, 1722–1734.
- (16) (a) Ahlström, B.; Chelminska-Bertilsson, M.; Thompson, R. A.; Edebo, L. *Antimicrob. Agents Chemother.* **1995**, *39*, 50–55. (b) Scherlund, M.; Brodin, A.; Malmsten, M. *J. Colloid Interface Sci.* **2000**, *229*, 365–374.
- (17) (a) Wen, X.; Franses, E. I. *J. Colloid Interface Sci.* **2000**, *231*, 42–51. (b) Groth, C.; Nydén, M.; Persson, K. C. *Langmuir* **2007**, *23*, 3000–3008.
- (18) Rehm, M.; Frank, M.; Schatz, J. *Tetrahedron Lett.* **2009**, *50*, 93–96.
- (19) It should be mentioned herein that 1:10 does not represent the host–guest binding stoichiometry, but is an optimized result for amphiphilic assembly by taking simultaneously the binding and assembly equilibria into account.
- (20) Lee, M.; Lee, S.-J.; Jiang, L.-H. *J. Am. Chem. Soc.* **2004**, *126*, 12724–12725.
- (21) (a) Hotz, J.; Meier, W. *Langmuir* **1998**, *14*, 1031–1036. (b) Egelhaaf, S. U.; Schertenberger, P. *J. Phys. Chem.* **1994**, *98*, 8560–8573. (c) Chécot, F.; Lecommandoux, S.; Gnanou, Y.; Klox, H.-A. *Angew. Chem., Int. Ed.* **2002**, *41*, 1339–1343.
- (22) Arena, G.; Contino, A.; Lombardo, G. G.; Sciotto, D. *Thermochim. Acta* **1995**, *264*, 1–11.